BIOCHEMISTRY
including biophysical chemistry & molecular biology

Article

pubs.acs.org/biochemistry

Specific Disruption of Transthyretin(105−115) Fibrilization Using "Stabilizing" Inhibitors of Transthyretin Amyloidogenesis

Yanfang Liang,[†] Moriam O. Ore,[†] Sylvie Morin,[†] and Derek J. Wilson*[,†,‡]

[†]Department of Chemistry and [‡]Center for Biomolecular Interactions, York University, Toronto, Ontario M3J 1P3, Canada

Supporting Information

ABSTRACT: Transthyretin (TTR) is a cerebrospinal fluid and serum protein that undergoes ordered aggregation (amyloidogenesis) in familial amyloidotic polyneuropathy (FAP) and senile systemic amyloidosis (SSA). It is now widely accepted that dissociation of the native TTR tetramer is a precondition for amyloidogenesis; thus, molecules that stabilize the tetramer have received much attention as potential TTR amyloidosis inhibitors. Many of these inhibitors bind to the thyroxine (T_4) binding pocket and interact specifically with a section of the TTR sequence, corresponding to residues 105−115, that is implicated in amyloidogenic propensity. In this work, we study the effects of "stabilizing" inhibitors on ordered aggregation of TTR(105−115) peptide. We show that molecules known to bind full-length TTR at the T_4 site are potent, specific inhibitors of ordered aggregation, while molecules that do not interact with TTR exhibit milder, nonspecific disruption through a "hyperbundling" effect. Our results suggest that, in addition to annealing the native tetramer, "stabilizing" inhibitors may also directly disrupt amyloidogenic aggregation of TTR monomers through specific interactions with the exposed TTR(105−115) sequence.

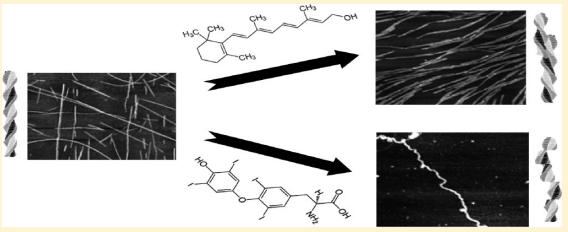

Amyloidosis is a pathogenic form of protein aggregation that is implicated in over 40 human illnesses including Alzheimer's disease, Parkinson's disease, type II diabetes, and Creutzfeldt−Jacob disease.[1−3] The pathological significance of amyloidosis has been recognized for more than 150 years; however, even with a recent surge in interest following the association with common neurodegenerative diseases, the mechanisms underlying amyloid formation remain poorly understood.[4,5] Consequently, progress in the development of effective antiamyloid drugs has been exceedingly slow. Current drug treatments for both neurodegenerative and systemic amyloidoses can temporarily improve quality of life but affect disease progression only slightly.[6,7]

One potential exception to this overall bleak picture are amyloidoses associated with the protein transthyretin (TTR), which include the most common systemic amyloidosis, FAP, and the late onset neurodegenerative disease SSA.[8,9] In its normal biological role, TTR acts as a carrier of T_4 in plasma and the cerebrospinal fluid. It also mediates retinol transport and uptake via specific interactions with retinol binding protein (RBP). The native configuration of TTR is a homotetramer with two T_4 binding sites located along one axis at the subunit interface (Figure 1).[10,11] It is well established that amyloidogenic propensity in TTR lies exclusively with the monomeric form of the protein; the homotetramer is completely nonamyloidogenic.[12−14] Thus, early onset TTR amyloidosis (associated with FAP) is linked to a range of tetramer-destabilizing single or double point mutations, of which around 80 have been identified thus far.[15]

Compounds that stabilize the TTR tetramer, on the other hand, are potent amyloidogenesis inhibitors and are often considered as potential drug treatments for TTR-associated amyloidoses.[16−20] Small molecules bound at the T_4 sites serve to "anneal" one of the interfacial axes, substantially increasing the stability of the tetramer overall.[16,21,22] Within the past two decades, a large number of these "stabilizing" inhibitors have

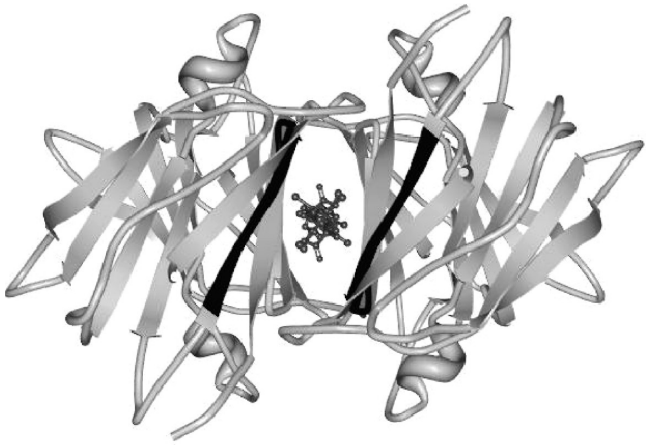

Figure 1. Image of the human TTR tetramer with T_4 bound (in the center). The view along the T_4 binding site axis to provides the best view of residues 105−115 (highlighted in black) in the T_4 binding pocket. Rendered from pdb file 2ROX[10] using PDB Protein Workshop v 3.9.[11]

Received: February 28, 2012
Revised: April 5, 2012
Published: April 6, 2012

 © 2012 American Chemical Society

been identified, including conventional nonsteroidal anti-inflammatory drugs (NSAIDs),[16] carborane cluster-containing NSAID derivatives,[17] and analogues of thyroxine such as biphenyl ethers,[19] benzoxazoles,[23] and "palindromic" thyroxin derivatives.[20] These molecules form a number of important contacts within the T_4 site. The termini typically interact with residues D54, K15, S117, and T119, and the diaryl core interacts with a cluster of residues including, T106, A108, A109, and L110.[18,24] Several T_4 mimetics are currently in clinical trials (including stage III) with promising results.

The ability of stabilizing inhibitors of TTR amyloidosis to pre-empt amyloidogenesis via stabilization of the TTR tetramer is well established *in vitro*.[16−19,25,26] In addition to the results from ongoing clinical trials, there is anecdotal evidence that TTR tetramer stabilization may be at least a moderately effective strategy *in vivo*, based on the fact that TTR is less amyloidogenic in the cerebrospinal fluid (CSF), where T_4 site occupancy is higher relative to the serum.[27] However, it is difficult to understand the basis of tetramer stabilizing inhibition in the context of low pH cellular compartments, which may be the origin of amyloidogenic TTR in the cell[27,28] and where even "stabilized" TTR tetramers would likely dissociate.[14]

With the focus on stabilization of the TTR tetramer, relatively little progress has been made in understanding the factors underlying amyloidogenic propensity in the monomeric protein. Some early work from Gustavsson and co-workers showed that two peptides forming β-strands within the T_4 binding site (amino acids 10−20 and 105−115 of the full-length TTR polypeptide) underwent amyloid-like aggregation *in vitro*.[29] Subsequent NMR-based analyses by Jaroniec et al. revealed that the structure adopted by TTR(105−115) in-fibril was an extended β-strand, similar to its configuration in native TTR as shown in Figure 1.[30,31] The amyloidogenic nature of TTR(105−115), together with the fact that this segment of the sequence becomes solvent exposed upon dissociation of the tetramer, would suggest that TTR(105−115) plays an important role in amyloidogenic aggregation of TTR monomers.

In this study, we investigate the ability of selected molecules to disrupt self-assembly of TTR(105−115) fibrils using a combination of saturation transfer difference (STD) NMR spectroscopy and imaging by atomic force microscopy (AFM) and scanning electron microscopy (SEM). Control molecules with no known interaction with TTR exhibit nonspecific perturbation of TTR(105−115) protofilament bundling, resulting in a branched, "hyperbundled" fibril morphology. In contrast, molecules that bind specifically at the T_4 site, including thyroxine and several NSAIDs, are potent inhibitors of ordered aggregation of TTR(105−115). Our results suggest that, in addition to stabilization of the TTR tetramer, "stabilizing" inhibitors may also directly disrupt amyloidogenesis of TTR monomers by specifically blocking access to the amyloidogenic TTR(105−115) segment.

EXPERIMENTAL PROCEDURES

Materials and Chemical Reagents. All small molecule inhibitors including L-thyroxine, flurbiprofen, flufenamic acid, diflunisal, retinol and acetaminophen were purchased from Sigma (St. Louis, MO). The peptides TTR(105−115) (Y-T-I-A-A-L-L-S-P-Y-S) and miniPEG-AALL were purchased from Biomatik Corp. (Cambridge, ON).

To test for inhibition activity, each of these molecules were dissolved in an "aggregation buffer" composed of HPLC grade water (Sigma), 10% (v/v) CD_3CN (Cambridge Isotope Laboratories Inc., Andover, MA), 0.1% (v/v) TFA (Sigma), and 10% (v/v) D_2O (Sigma). The final pH was 2.0. The solutions were then filtered using 0.1 μm nylon syringe filers (Fisher Canada, Ottawa, ON) to obtain the maximum soluble concentration of low solubility inhibitors (i.e., L-thyroxine, flurbiprofen, flufenmaic acid, diflunisal, biotin, and retinol), which was typically between 1 and 10 μM. The maximum concentrations of soluble inhibitors acetaminophen and miniPEG-AALL used were 1 mM and 500 μM, respectively. In concentration dependence experiments, these solutions were diluted with "blank" aggregation buffer.

Ordered aggregation was initiated by adding lyophilized TTR(105−115) to a concentration of 1.2 mM, allowing ∼2 h for solvation, and then refiltering with 0.1 μm nylon syringe filters. We found this method to yield 1 mM soluble TTR(105−115) (measured using tyrosine absorption, ε_0 = 2800 at λ = 274 nm) with no aggregates detected in initial AFM images. Then the final sample solutions were collected directly into 5 mm Norell NMR tubes (Chemglass, Vineland, NJ) for analysis. Samples were aged at room temperature for ∼3 weeks, during which time NMR experiments were conducted and aliquots were withdrawn periodically for AFM experiments.

Saturation Transfer NMR. All NMR data were collected using Bruker DRX 600 MHz spectrometer at 25 °C. Water suppression was implemented using excitation sculpting with gradients.[32] The pulse sequence for the STD NMR experiments was employed as previously described.[33] Briefly, a train of 60 Gian-shaped pulses at 40 dB and 12 ms duration separated by a 1 ms delay was applied to achieve selective saturation. Off-resonance irradiation for the saturation transfer reference spectra was performed at 25 ppm. On-resonance irradiation was performed at 0 ppm for the saturation transfer experiments. This differs somewhat from conventional STD-NMR experiments in which a specific, detectable resonance on the target molecule is saturated. In our case, the size of the TTR(105−115) fibrils (≫100 kDa) results in extreme broadening of the resonances associated with in-fibril TTR(105−115), while the peaks associated with the soluble species remain sharp. This allows us to selectively saturate a fraction of the in-fibril protons at virtually *any* chemical shift (though not as far downfield as 25 ppm where we apply the saturation pulse in off-resonance spectra). Saturation spreads rapidly throughout the fibril via dipolar couplings, which can then be transferred to soluble TTR on binding. Control experiments were performed to ensure no direct saturation of soluble TTR(105−115) in "on-resonance" experiments.

Saturation transfer efficiency was determined by measuring the ratio of the intensity of the on- and off-resonance difference spectrum I_{STD} to the off resonance spectrum I_{STR} at each peak. To compare the degree of the saturation, I_{STD}/I_{STR} values were normalized to the highest STD efficiency I^{max}_{STD}/I_{STR}.[34]

2D NMR Experiments. 2D total correlation spectroscopy (TOCSY) pulse sequence was implemented using the DIPSI-2 sequence for mixing.[35] The isotropic mixing time was 80 ms. The spectral width was 6.6 kHz in both dimensions. Spectra were 2048 points in the direct dimension for each of 128 increments in the indirect dimension (256 transients/increment) with quadrature detection by States-TPPI. All NMR data were processed using the MestRe Nova program (Mestrelab Research, Santiago de Compostela, Spain).

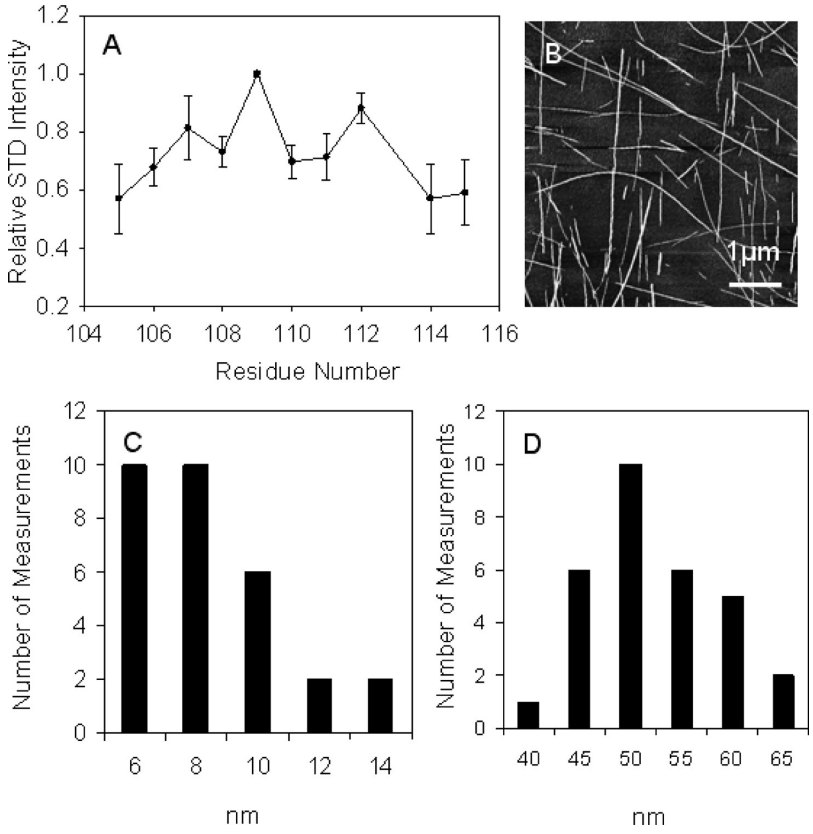

Figure 2. STD and AFM analysis of unperturbed TTR(105−115) fibrils. (A) STD profile for backbone amide protons of TTR(105−115) after 3 weeks of incubation, corresponding to the midpoint of ordered aggregation. Error bars are the standard deviation from 5 transients. (B) AFM image (5 × 5 μm) showing unperturbed TTR(105−115) fibril morphology. (C, D) Statistical analysis of fibril height and width (respectively), based 30 randomly sampled measurements.

Atomic Force and Electron Microscopy. AFM imaging was performed using a Dimension 3100 scanning probe microscope (SPM) from Veeco (Peabody, MA) with 125 μm silicon SPM tip with a spring constant of 37.09 N/m which was purchased from Digital Instruments (Santa Barbara, CA). All AFM experiments were conducted in air. After incubation, samples were extracted directly from NMR tubes, diluted 2−4 times in aggregation buffer and applied to a freshly cleaved mica substrate, and then allowed 2 min for adsorption. The same procedure was applied for sample in the later stages of ordered aggregation, but with 5−10-fold dilution. After sample deposition, the substrate was washed with the HPLC grade water and dried with argon gas (Air Liquide, Burlington, ON). Imaging was carried out in tapping mode. The scan speed was 1.00 or 1.5 Hz. The drive amplitude of 200−973.4 mV and resonant frequency of 298−300 Hz were employed. Images were analyzed and measurments taken using the Image SXM software package.[36] Length and width distributions were derived from 30 randomly sampled measurements per image.

Electron micrographs were generated using a Hitachi S-520 scanning electron microscope. Samples were deposited on a carbon-coated EM grid and dried by desiccation under low vacuum for 10 min. Dried samples were subjected to negative staining using 1% phosphotungstic acid, followed by a second round of desiccation prior to imaging.

■ RESULTS AND DISCUSSION

Ordered Aggregation of TTR(105−115). TTR(105−115) is among the most well-characterized models of ordered aggregation. The smallest ordered aggregates of TTR(105−115) (protofibrils) are thought to be single layer β-sheets composed of "in register" parallel strands.[31,37] Protofibrils stacked in an antiparallel arrangement correspond to a protofilament. A mature fibril consists of approximately four intertwined protofilaments.[38] To provide a baseline for our subsequent experiments, we first generated fibrils of TTR(105−115) in the absence of small-molecule inhibitors. 1D STD NMR spectroscopy was used to probe the binding configuration of soluble TTR(105−115) to fibrillar TTR(105−115).[39,40] Raw NMR spectra corresponding to a typical STD-NMR experiment are shown in Figure S1 with an arrow indication the position of the saturation pulse. The underlying principle of this experiment is that saturation transfer efficiency decreases with increasing distance between saturated and unsaturated atoms during a binding event.[39] Thus, specific binding configurations yield unique "STD profiles" (e.g., Figure 2A) in which the intermolecular binding mode is reflected in the degree of saturation of specific atoms. The backbone amide proton STD profile shown in Figure 2A, which was collected roughly at the midpoint of the aggregation process, is consistent with those reported previously by our group.[33,41]

We use AFM and SEM imaging to reveal the consequences of altered intermolecular interactions on fibril morphology. Figure 2B represents the classic TTR(105−115) fibril structure consisting of long, unbranched strands. Morphological details, including height and width distributions, are provided in Figure 2C,D. These measurements are consistent with those reported

dx.doi.org/10.1021/bi3002727 | Biochemistry 2012, 51, 3523−3530

previously[33] showing a "flattening" of the fibrils as they are adsorbed onto the mica surface.

Nonspecific Inhibitors. As a negative control, we tested the effect of several molecules that are not known to interact directly with TTR on TTR(105−115) ordered aggregation. Retinol is associated with TTR indirectly, through the interaction between TTR and RBP.[27] A very recent study by Hyung et al. showed that some retinoids, but *not* retinol, were capable of stabilizing the TTR tetramer even in the absence of RBP, suggesting a direct interaction with the protein.[42] In the present study, retinol was selected as a TTR-relevant molecule that does not bind the T_4-site and hence should not interact specifically with TTR(105−115). Neither Retinol nor any of the other nonspecific inhibitors tested induced a chemical shift change or line broadening in the TTR(105−115) ^{1}H spectrum, suggesting no significant interaction between these molecules and the soluble peptide.

In the presence of retinol and after 48 h of incubation, STD experiments yield an unambiguous profile for TTR(105−115) amide protons, which is indicative of a specific binding mode and thus ordered aggregation (Figure 3A). Overall, the profile

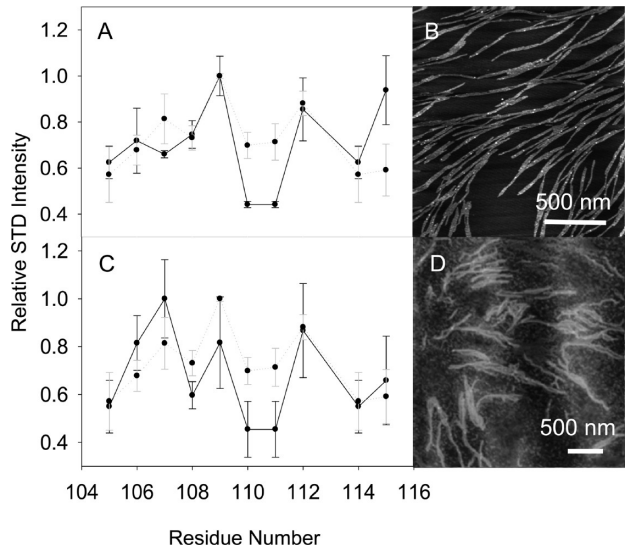

Figure 3. STD and AFM analysis of TTR(105−115) ordered aggregation in the presence of nonspecific inhibitors. (A) The STD profile for the amide protons of TTR(105−115) after 48 h incubation in the presence of retinol, corresponding to the maximum population of hyperbundled fibrils. Error bars are the standard deviation from 5 transients. The native STD profile is provided for comparison (gray outline circles, dotted line). (B) Typical AFM image (2 × 2 μm) of hyperbundled TTR(105−115) fibrils after 48 h incubation in the presence of 1.7 μM retinol. (C) The STD profile for the amide protons of TTR(105−115) after 48 h incubation in the presence of 116 μM acetaminophen. Error bars are the standard deviation from 5 transients. (D) Typical AFM image (3 × 3 μm) showing hyperbundled TTR(105−115) aggregates in the presence of 116 μM acetaminophen.

is similar to that of TTR(105−115) in the absence of retinol (shown in gray), except for a substantially more pronounced "dip" at Leu 110 and Leu 111. This reduced saturation transfer efficiency in the amide backbone is correlated with an increased saturation of C_β side-chain protons on the same residues (data not shown), which we interpret to indicate close aliphatic interactions with the fibril on binding.[33] The significantly increased amide proton saturation at Ser 115 may reflect a slightly altered binding configuration in which the Ser 115 backbone hydrogen is in close proximity to the fibril on binding.

AFM images collected after 48 h of incubation revealed a "branched" fibril morphology (Figure 3B).[43] Upon analysis of the AFM data, it is clear that the "branching" is not due to forking of the growing ends, but rather perturbed bundling. Fibril widths immediately prior to branchpoints are 75 ± 6 nm on average, substantially wider than the 52 ± 4 nm average for unperturbed TTR fibrils (Figure 2C). The average width of fibrils immediately after branchpoints is comparable to unperturbed fibrils (43 ± 6 nm). This would suggest a "hyperbundled" morphology in which an excessive number of protofilaments are recruited into fibrils, with periodic unbundling once a critical diameter is reached. Hyperbundling agrees well with the detection of increased saturation of C_β protons on Leu 110 and Leu 111 as this feature of the STD profile was linked previously to the incorporation of soluble TTR(105−115) into mature, bundled fibrils.[33] Hyperbundling has also been observed for a different amyloidogenic species ($A\beta_{1-40}$) in the presence of a different small molecule (Congo Red),[44] supporting the hypothesis that it is a nonspecific phenomenon. Hyperbundled TTR(105−115) fibrils lack the stability of unperturbed fibrils, decaying completely to amorphous aggregates after ∼96 h of incubation.

We also monitored TTR(105−115) fibrilization in the presence of acetaminophen, which is functionally related to NSAIDs but not known to interact specifically with TTR. Acetaminophen is substantially more soluble than retinol under our conditions, allowing us to examine nonspecific disruption at stoichiometric concentrations of inhibitor. For acetaminophen concentrations at and above 1 mM, there was a substantial decrease in signal-to-noise in the raw STD spectrum. There is therefore an increased uncertainty in the STD profile (Figure 3C), though lower backbone amide proton saturation at Leu 110 and Leu 111 is still detectable, as is the concomitant increase in the C_β protons (data not shown). In previous work, similar decreases in signal-to-noise were linked to concurrent ordered and disordered aggregation.[41] The STD profile acquired in the presence of acetaminophen agrees with the unperturbed profile at Ser 115 but shows significantly increased saturation at Ile 107. This would suggest a distinct binding configuration with closer positioning of the Ile 107 backbone amide proton to the fibril.

As predicted from the decrease in STD signal-to-noise, corresponding AFM images reveal intensely hyperbundled fibrils together with substantial amorphous aggregation (Figure 3D). While the occurrence of hyperbundling appears independent of the nonspecific inhibitor used, the *extent* of hyperbundling was influenced both by the nature of the inhibitor and its concentration. For example, acetaminophen was a significantly weaker hyperbundling agent than retinol, requiring ∼50-fold higher concentration to a produce the same degree of "branching". Biotin was also tested and found to have a hyperbundling propensity similar to retinol. It is likely that the most important factor dictating hyperbundling propensity is solubility, since this parameter would directly influence degree of nonspecific interaction with the fibril.

Specific Inhibitors. In order to test for specific inhibition of TTR(105−115) ordered aggregation, we selected molecules known to interact with TTR at the T_4 binding site. These included T_4 and NSAIDs flurbiprophen, diflunisal, and flufenamic acid. We also tested a solubility tagged tetrapeptide (miniPEG-A-A-L-L) corresponding to the "binding core" of

dx.doi.org/10.1021/bi3002727 | *Biochemistry* 2012, 51, 3523−3530

TTR(105−115).[33,45] All of these molecules exhibited complete inhibition of ordered aggregation under our conditions, even at >1000-fold dilutions relative to TTR(105−115) (i.e., nanomolar concentrations of the inhibitor). It would be hard to attribute this level of potency to a nonspecific interaction with the fibril, but in the case of a specific inhibitor, it can be rationalized by arguing that the compound acts specifically on the growing fibril *ends*, which would be orders of magnitude lower in concentration than the peptide itself (mid-nanomolar range).[46]

Saturation transfer cannot be used in the absence of ordered aggregation because a singular binding mode is required to generate distinctive features in the STD profile (although nonspecific saturation transfer still occurs through disordered interactions). Figure 4A shows a TTR(105−115) STD "profile"

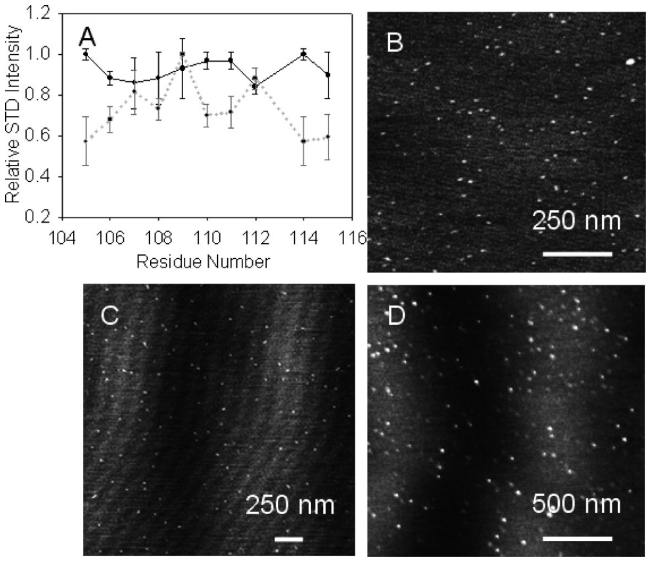

Figure 4. STD and AFM analysis of TTR(105−115) aggregation in the presence of specific inhibitors. (A) Typical STD "profile" associated with pure amorphous aggregation. These data were acquired in the presence of thyroxine at its solubility limit (10 μM). Error bars are from 5 transients. The native STD profile is provided for comparison (gray outline circles, dotted line). (B) (C), and (D) are AFM images showing the amorphous aggregates that form in the presence of specific inhibitors thyroxine (10 μM), flurbiprophen (10 nM), and miniPEG-A-A-L-L (10 nM), respectively. Flurbiprophen and miniPEG-A-A-L-L are shown at the lowest concentration for which amorphous aggregates were observed. Further dilutions of all specific inhibitors (to 5 and 1 nM) resulted in unperturbed ordered aggregation.

collected in the presence of T_4 at its solubility limit (10 μM). The increased uncertainty and "flattening" of the profile are typical of pure amorphous aggregation.[41] Figures 4B−D show AFM images of amorphous aggregation in the presence of T_4, flurbiprofen, and miniPEG-A-A-L-L, respectively. These aggregates differ somewhat in size but are clearly exclusively amorphous.

In order to reveal the underlying mechanism of specific inhibition, we searched for a concentration regime in which ordered aggregation was only partially disrupted by a specific inhibitor. This proved to be exceedingly difficult for all molecules tested due to a sharp boundary between complete inhibition and unperturbed ordered aggregation at ~10 nM inhibitor. However, in the case of T_4, conditions were found in which concurrent ordered and amorphous aggregation were observed. AFM images from a series of T_4 dilutions are shown in Figure 5. At 10 μM T_4, the aggregates are small and spherical, which is typical of pure amorphous aggregation (Figure 5A). In the presence 100 nM T_4 the aggregates are still clearly amorphous but are now larger and nonspherical (Figure 5B). These aggregates bear a resemblance to the "seed clusters" that are often observed in early fibril formation *in vitro*;[43,44]

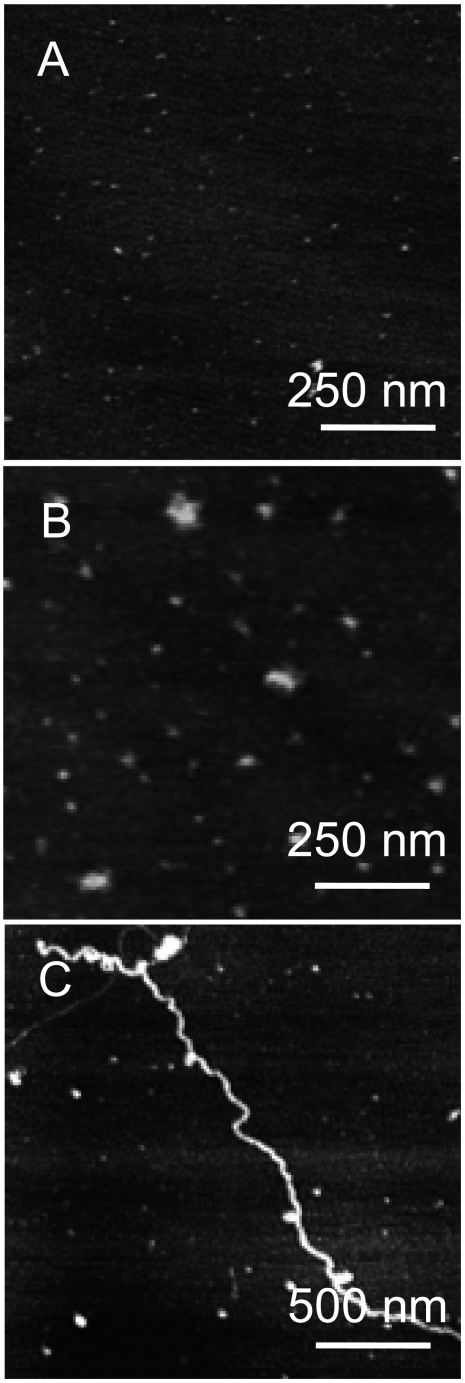

Figure 5. AFM images showing the concentration dependence for specific inhibition of TTR(105−115) ordered aggregation by thyroxine. All images were acquired after 3 weeks incubation with TTR(105−115) concentration 1 mM. (A) Thyroxine concentration at its solubility limit (10 μM). (B) 100-fold dilution (100 nM). (C) 1000-fold dilution (10 nM).

dx.doi.org/10.1021/bi3002727 | *Biochemistry* 2012, 51, 3523−3530

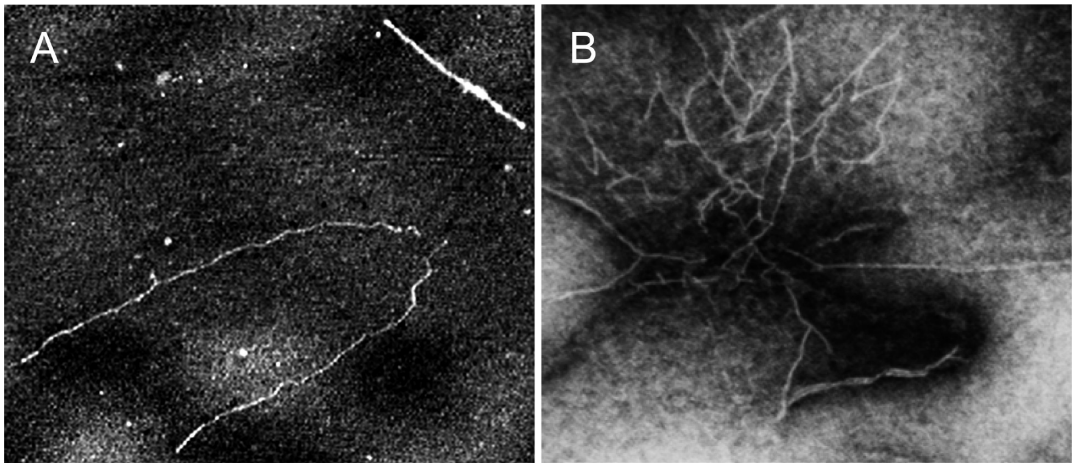

Figure 6. Images of DFNKF fibrils in the presence and absence of T_4. (A) Native DFNKF fibrils in the absence of T_4 (3 × 3 μm). (B) Fibrils generated in the presence of 10 μM T_4 (3 × 3 μm).

however, no fibrils were observed at this dilution even after several months of incubation.

At 10 nM of T_4, TTR(105−115) fibrils were observed (Figure 5C), though amorphous aggregation was still dominant, preventing a meaningful analysis by STD. Limited specific disruption of ordered aggregation is evident nonetheless in the adoption of a "kinked" morphology that is substantially different from unperturbed fibrils. In contrast to hyperbundling in nonspecific inhibition, the "kinked" morphology is suggestive of direct interference with the incorporation of soluble TTR(105−115) into lengthening fibrils, most likely through blocking of exposed TTR(105−115) binding cores (i.e., A_{108}-A_{109}-L_{110}-L_{111})[45] at the growing fibril ends. Thus, specific inhibitors tip the balance between ordered and amorphous aggregation[47] by interposing themselves between fibrillar aggregate attachment sites and soluble TTR(105−115). This model for disruption is consistent with both the high potency of specific inhibitors and the abrupt transition between pure amorphous and fully ordered aggregation in dilution experiments.

Specificity of T_4 Inhibition for TTR(105−115). While molecules that bind the T_4 site of TTR clearly exhibit enhanced inhibition of ordered aggregation for TTR(105−115), it is possible that these compounds are potent disruptors of amyloid-like aggregation in general. Studies comparing serum levels of free T_4 to the volume of Alzheimer's-linked amyloid deposits (i.e., neocortical neuritic plaques of *A*-beta and neurofibrillary tangles of tau protein) suggest that, far from exhibiting an inhibitory effect, high levels of free T_4 actually *intensify* amyloidogensis *in vivo*.[48,49] For additional evidence *in vitro*, we monitored fibrilization of another model peptide, DFNKF, in the presence and absence of T_4 (Figure 6). This molecule was selected for its TTR(105−115)-like aggregation mechanism and supramolecular structure.[50] As can be seen in Figure 6B, DFNKF underwent extensive fibrilization even in the presence of relatively high concentrations of T_4 (up to its 10 μM solubility limit). As with nonspecific inhibition of TTR(105−115) fibrilization, fibril branching in Figure 6B is consistent with *nonspecific* interactions between T_4 and growing DFNKF fibrils.

CONCLUSIONS

In summary, we have demonstrated that compounds known to bind the T_4 site of TTR are potent, specific inhibitors of ordered aggregation in an amyloidogenic segment of the full-length protein, TTR(105−115). Compounds selected as negative controls also inhibited fibrillization at higher concentrations, but through a nonspecific mechanism involving perturbation of protofilament bundling. These data suggest that even in the event of complete monomerization of TTR (e.g., in low pH cellular compartments), stabilizing inhibitors may still disrupt amyloidogenesis by specifically blocking the exposed amyloidogenic segment TTR(105−115).

Clearly, it will be desirable in future work to acquire direct evidence that this "blocking" mechanism applies equally to aggregation of the full-length protein. However, in the presence of the native tetramer, such studies will be complicated by the dual antiamyloidogenic mechanisms of specific inhibitors; i.e., it will be challenging to separate effects due to tretramer stabilization from effects due to amyloidogenic epitope blocking. One option may be to use a mutant that strongly destabilizes the tetramer so that the protein is essentially completely monomeric in spite of the presence of a "stabilizing" inhibitor; however, those strongly destabilizing mutants that have been developed thus far are weakly amyloidogenic under native conditions.[51,52] Natively folded monomers of the moderately amyloidogenic variant TTR(T119M) have been transiently generated via a subdenaturing pulse of urea and high hydrostatic pressure.[51]

ASSOCIATED CONTENT

Supporting Information

Raw spectra from a typical STD experiment including both on- and off-resonance experiments. This material is available free of charge via the Internet at http://pubs.acs.org.

AUTHOR INFORMATION

Corresponding Author

*Tel +1 (416) 736-2100 x20786; e-mail dkwilson@yorku.ca.

Funding

Funding for this research was provided by the Natural Science and Engineering Research Council of Canada (NSERC) Discovery Grant program.

Notes

The authors declare no competing financial interest.

■ ACKNOWLEDGMENTS

The authors thank Howard Hunter for technical assistance with the NMR experiments and helpful discussions.

■ REFERENCES

(1) Plakoutsi, G., Bemporad, F., Monti, M., Pagnozzi, D., Pucci, P., and Chiti, F. (2006) Exploring the mechanism of formation of native-like and precursor amyloid oligomers for the native acylphosphatase from Sulfolobus solfataricus. *Structure 14*, 993−1001.

(2) Pepys, M. B. (2006) Amyloidosis. *Annu. Rev. Med. 57*, 223−241.

(3) Carrell, R. W., and Lomas, D. A. (1997) Conformational disease. *Lancet 350*, 134−138.

(4) Bellotti, V., and Chiti, F. (2008) Amyloidogenesis in its biological environment: challenging a fundamental issue in protein misfolding diseases. *Curr. Opin. Struct. Biol. 18*, 771−779.

(5) Uversky, V. N. (2010) Mysterious oligomerization of the amyloidogenic proteins. *FEBS J. 277*, 2940−2953.

(6) Citron, M. (2010) Alzheimer's disease: strategies for disease modification. *Nat. Rev. Drug Discovery 9*, 387−398.

(7) Skinner, M., Anderson, J. J., Simms, R., Falk, R., Wang, M., Libbey, C. A., Jones, L. A., and Cohen, A. S. (1996) Treatment of 100 patients with primary amyloidosis: A randomized trial of melphalan, prednisone and colchicine versus colchicine only. *Am. J. Med. 100*, 290−298.

(8) Lee, K. W., Lee, D. H., Son, H., Kim, Y. S., Park, J. Y., Roh, G. S., Kim, H. J., Kang, S. S., Cho, G. J., and Choi, W. S. (2009) Clusterin regulates transthyretin amyloidosis. *Biochem. Biophys. Res. Commun. 388*, 256−260.

(9) Ando, Y., Nakamura, M., and Araki, S. (2005) Transthyretin-related familial amyloidotic polyneuropathy. *Arch. Neurol. 62*, 1057−1062.

(10) Wojtczak, A., Cody, V., Luft, J. R., and Pangborn, W. (1996) Structures of human transthyretin complexed with thyroxine at 2.0 angstrom resolution and 3′,5′-dinitro-N-acetyl-L-thyronine at 2.2 angstrom resolution. *Acta Crystallogr., Sect. D: Biol. Crystallogr. 52*, 758−765.

(11) Moreland, J. L., Gramada, A., Buzko, O. V., Zhang, Q., and Bourne, P. E. (2005) The Molecular Biology Toolkit (MBT): A Modular Platform for Developing Molecular Visualization Applications. *BMC Bioinf. 6*, 11.

(12) Lai, Z. H., Colon, W., and Kelly, J. W. (1996) The acid-mediated denaturation pathway of transthyretin yields a conformational intermediate that can self-assemble into amyloid. *Biochemistry 35*, 6470−6482.

(13) Hurshman, A. R., White, J. T., Powers, E. T., and Kelly, J. W. (2004) Transthyretin aggregation under partially denaturing conditions is a downhill polymerization. *Biochemistry 43*, 7365−7381.

(14) McCutchen, S. L., Colon, W., and Kelly, J. W. (1993) Transthyretin mutation Leu-55-Pro significantly alters tetramer stability and increases amyloidogenicity. *Biochemistry 32*, 12119−12127.

(15) Connors, L. H., Lim, A., Prokaeva, T., Roskens, V. A., and Costello, C. E. (2003) Tabulation of human transthyretin (TTR) variants. *Amyloid 10*, 160−184.

(16) Peterson, S. A., Klabunde, T., Lashuel, H. A., Purkey, H., Sacchettini, J. C., and Kelly, J. W. (1998) Inhibiting transthyretin conformational changes that lead to amyloid fibril formation. *Proc. Natl. Acad. Sci. U. S. A. 95*, 12956−12960.

(17) Julius, R. L., Farha, O. K., Chiang, J., Perry, L. J., and Hawthorne, M. F. (2007) Synthesis and evaluation of transthyretin amyloidosis inhibitors containing carborane pharmacophores. *Proc. Natl. Acad. Sci. U. S. A. 104*, 4808−4813.

(18) Palaninathan, S. K., Mohamedmohaideen, N. N., Orlandini, E., Ortore, G., Nencetti, S., Lapucci, A., Rossello, A., Freundlich, J. S., and Sacchettini, J. C. (2009) Novel Transthyretin Amyloid Fibril Formation Inhibitors: Synthesis, Biological Evaluation, and X-Ray Structural Analysis. *PLoS One 4*, 15.

(19) Gupta, S., Chhibber, M., Sinha, S., and Surolia, A. (2007) Design of mechanism-based inhibitors of transthyretin amyloidosis: Studies with biphenyl ethers and new structural templates. *J. Med. Chem. 50*, 5589−5599.

(20) Kolstoe, S. E., Mangione, P. P., Bellotti, V., Taylor, G. W., Tennent, G. A., Deroo, S., Morrison, A. J., Cobb, A. J. A., Coyne, A., McCammon, M. G., Warner, T. D., Mitchell, J., Gill, R., Smith, M. D., Ley, S. V., Robinson, C. V., Wood, S. P., and Pepys, M. B. (2010) Trapping of palindromic ligands within native transthyretin prevents amyloid formation. *Proc. Natl. Acad. Sci. U. S. A. 107*, 20483−20488.

(21) Damas, A. M., and Saraiva, M. J. (2000) Review: TTR amyloidosis - Structural features leading to protein aggregation and their implications on therapeutic strategies. *J. Struct. Biol 130*, 290−299.

(22) McCammon, M. G., Scott, D. J., Keetch, C. A., Greene, L. H., Purkey, H. E., Petrassi, H. M., Kelly, J. W., and Robinson, C. V. (2002) Screening transthyretin amyloid fibril inhibitors: Characterization of novel multiprotein, multiligand complexes by mass spectrometry. *Structure 10*, 851−863.

(23) Razavi, H., Palaninathan, S. K., Powers, E. T., Wiseman, R. L., Purkey, H. E., Mohamedmohaideen, N. N., Deechongkit, S., Chiang, K. P., Dendle, M. T. A., Sacchettini, J. C., and Kelly, J. W. (2003) Benzoxazoles as Transthyretin Amyloid Fibril Inhibitors: Synthesis, Evaluation, and Mechanism of Action. *Angew. Chem. 115*, 2864−2867.

(24) Choi, S., Reixach, N., Connelly, S., Johnson, S. M., Wilson, I. A., and Kelly, J. W. (2010) A Substructure Combination Strategy To Create Potent and Selective Transthyretin Kinetic Stabilizers That Prevent Amyloidogenesis and Cytotoxicity. *J. Am. Chem. Soc. 132*, 1359−1370.

(25) Miroy, G. J., Lai, Z. H., Lashuel, H. A., Peterson, S. A., Strang, C., and Kelly, J. W. (1996) Inhibiting transthyretin amyloid fibril formation via protein stabilization. *Proc. Natl. Acad. Sci. U. S. A. 93*, 15051−15056.

(26) Reixach, N., Adamski-Werner, S. L., Kelly, J. W., Koziol, J., and Buxbaum, J. N. (2006) Cell based screening of inhibitors of transthyretin aggregation. *Biochem. Biophys. Res. Commun. 348*, 889−897.

(27) Buxbaum, J. N., and Reixach, N. (2009) Transthyretin: the servant of many masters. *Cell. Mol. Life Sci. 66*, 3095−3101.

(28) Lashuel, H. A., Lai, Z. H., and Kelly, J. W. (1998) Characterization of the transthyretin acid denaturation pathways by analytical ultracentrifugation: Implications for wild-type, V30M, and L55P amyloid fibril formation. *Biochemistry 37*, 17851−17864.

(29) Gustavsson, A., Engstrom, U., and Westermark, P. (1991) Normal Transthyretin and Sythetic Transthyretin Fragments Form Amyloid-like Fibrils in Vitro. *Biochem. Biophys. Res. Commun. 175*, 1159−1164.

(30) Jaroniec, C. P., MacPhee, C. E., Astrof, N. S., Dobson, C. M., and Griffin, R. G. (2002) Molecular Conformation of a Peptide Fragment of Transthyretin in an Amyloid Fibril. *Proc. Natl. Acad. Sci. U. S. A. 99*, 16748−16753.

(31) Jaroniec, C. P., MacPhee, C. E., Bajaj, V. S., McMahon, M. T., Dobson, C. M., and Griffin, R. G. (2004) High-resolution Molecular Structure of a Peptide in an Amyloid Fibril Determined by Magic Angle Spinning NMR Spectroscopy. *Proc. Natl. Acad. Sci. U. S. A. 101*, 711−716.

(32) Hwang, T. L., and Shaka, A. J. (1995) Water Suppression That Works. Excitation Sculpting Using Arbitrary Wave-Forms and Pulsed-Field Gradients. *J. Magn. Reson. A 112*, 275−279.

(33) Liang, Y. F., Jasbi, S. Z., Haftchenary, S., Morin, S., and Wilson, D. J. (2009) Binding interactions in early- and late-stage amyloid aggregates of TTR(105−115). *Biophys. Chem. 144*, 1−8.

(34) Milojevic, J., Raditsis, A., and Melacini, G. (2009) Human Serum Albumin Inhibits A beta Fibrillization through a "Monomer-Competitor" Mechanism. *Biophys. J. 97*, 2585−2594.

(35) Rucker, S. P., and Shaka, A. J. (1989) Broad-Band Homonuclear Cross-Polarization in 2D NMR Using DIPSI-2. *Mol. Phys. 68*, 509−517.
(36) Barrett, S. D. (2008) *Image SXM*, http://www.ImageSXM.org.uk.
(37) Deng, W., Cao, A., and Lai, L. (2007) Detecting the interpeptide arrangement and maturation process of transthyretin (105−115) amyloid fibril using a FRET pair with short Förster distance. *Biochem. Biophys. Res. Commun. 362*, 689−694.
(38) Mesquida, P., Riener, C. K., MacPhee, C. E., and McKendry, R. A. (2007) Morphology and mechanical stability of amyloid-like peptide fibrils. *J. Mater. Sci., Mater. Med. 18*, 1325−1331.
(39) Mayer, M., and Meyer, B. (2001) Group epitope mapping by saturation transfer difference NMR to identify segments of a ligand in direct contact with a protein receptor. *J. Am. Chem. Soc. 123*, 6108−6117.
(40) Huang, H., Milojevic, J., and Melacini, G. (2008) Analysis and optimization of saturation transfer difference NMR experiments designed to map early self-association events in amyloidogenic peptides. *J. Phys. Chem. B 112*, 5795−5802.
(41) Liang, Y. F., Jasbi, S. Z., Morin, S., and Wilson, D. J. (2010) Rational Manipulation of Amyloidogenesis Using an Atomic Level Map of Peptide-Fibril Interactions. *Biochemistry 49*, 5829−5831.
(42) Hyung, S. J., Deroo, S., and Robinson, C. V. (2010) Retinol and Retinol-Binding Protein Stabilize Transthyretin via Formation of Retinol Transport Complex. *ACS Chem. Biol. 5*, 1137−1146.
(43) Andersen, C. B., Yagi, H., Manno, M., Martorana, V., Ban, T., Christiansen, G., Otzen, D. E., Goto, Y., and Rischel, C. (2009) Branching in Amyloid Fibril Growth. *Biophys. J. 96*, 1529−1536.
(44) Bose, P. P., Chatterjee, U., Xie, L., Johansson, J., Gothelid, E., and Arvidsson, P. I. (2010) Effects of Congo Red on A beta(1−40) Fibril Formation Process and Morphology. *ACS Chem. Neurosci. 1*, 315−324.
(45) Paci, E., Gsponer, J., Salvatella, X., and Vendruscolo, M. (2004) Molecular dynamics studies of the process of amyloid aggregation of peptide fragments of transthyretin. *J. Mol. Biol. 340*, 555−569.
(46) Bongiovanni, M. N., Puri, D., Goldie, K. N., and Gras, S. L. (2012) Noncore Residues Influence the Kinetics of Functional TTR105−115-Based Amyloid Fibril Assembly. *J. Mol. Biol.*, DOI: 10.1016/j.jmb.2011.12.020.
(47) O'Nuallain, B., Thakur, A. K., Williams, A. D., Bhattacharyya, A. M., Chen, S., Thiagarajan, G., Wetzel, R., Kheterpal, I., and Ronald, W. (2006) Kinetics and Thermodynamics of Amyloid Assembly Using a High-Performance Liquid Chromatography-Based Sedimentation Assay, in *Methods in Enzymology*, pp 34−74, Academic Press, New York.
(48) de Jong, F. J., Masaki, K., Chen, H., Remaley, A. T., Breteler, M. M. B., Petrovitch, H., White, L. R., and Launer, L. J. (2009) Thyroid function, the risk of dementia and neuropathologic changes: The Honolulu−Asia Aging Study. *Neurobiol. Aging 30*, 600−606.
(49) Stuerenburg, H. J., Arlt, S., and Mueller-Thomsen, T. (2006) Free thyroxine, cognitive decline and depression in Alzheimer's disease. *Neuroendocrinol. Lett. 27*, 535−537.
(50) Reches, M., Porat, Y., and Gazit, E. (2002) Amyloid fibril formation by pentapeptide and tetrapeptide fragments of human calcitonin. *J. Biol. Chem. 277*, 35475−35480.
(51) Palhano, F. L., Leme, L. P., Busnardo, R. G., and Foguel, D. (2009) Trapping the Monomer of a Non-amyloidogenic Variant of Transthyretin: Exploring its possible use as a therapeutic strategy against transthyretin amyloidogenic diseases. *J. Biol. Chem. 284*, 1443−1453.
(52) Jiang, X., Smith, C. S., Petrassi, H. M., Hammarstrom, P., White, J. T., Sacchettini, J. C., and Kelly, J. W. (2001) An engineered transthyretin monomer that is nonamyloidogenic, unless it is partially denatured. *Biochemistry 40*, 11442−11452.